

A STUDY OF THE LONGITUDINAL LOW FREQUENCY
(PHUGOID) MOTION OF AN AIRPLANE
AT SUPERSONIC AND HYPERSONIC SPEEDS

Thesis by
Uso Walter

In Partial Fulfillment of the Requirements
For the Degree of
Aeronautical Engineer

California Institute of Technology

Pasadena, California

1967

(Submitted May 26, 1967)

ACKNOWLEDGMENTS

The author wishes to thank Professor H. J. Stewart for the valuable assistance given by him as research advisor and Professor P. Lissaman for his helpful criticism and suggestions.

The author further feels indebted to the National Aeronautics and Space Administration and to the government of the Federal Republic of Germany for fellowship support under the NASA International Fellowship Program and to Dean S. S. Steinberg, National Academy of Sciences, National Research Council, for his extremely personal, openminded, and unbureaucratic administration of the fellowship program.

ABSTRACT

The character of the longitudinal low frequency (phugoid) motion of a rigid airplane with controls fixed is investigated for the flight Mach number range from 1.25 to 8.0 using the physical and aerodynamic data of the North American X-15 research airplane.

The validity of the simplifying assumptions made in most low speed airplane stability investigations (symmetry of the airplane and of the air flow, small perturbations) is established for the problem under consideration.

The equations of longitudinal motion have been solved for the flight altitudes: sea level, 20,000 ft., 40,000 ft., and 60,000 ft.; and in addition the roots of the simplified equations resulting from the phugoid approximation have been calculated for the same flight situations. It is found that the deviation of these approximate solutions from the solutions of the complete longitudinal equations is below 5 per cent throughout the considered range of flight conditions, and for most calculated points is less than 2 per cent. The phugoid roots are complex at 60,000 ft. altitude and real at sea level, with transition from one mode to the other at the intermediate flight altitudes. The real part of the roots is always negative, i. e., there is no divergence of the motion. Using the phugoid approximation, a criterion for the degeneration of the periodic phugoid mode into aperiodic modes is derived in form of a critical value of the lift to drag ratio C_L/C_D .

In an appendix, the influence of an additional damping force (thrust control by the auto-pilot) on the character of the phugoid roots is shown.

TABLE OF CONTENTS

<u>Part</u>	<u>Title</u>	<u>Page</u>
	Acknowledgments	ii
	Abstract	iii
	Table of Contents	iv
I.	INTRODUCTION	1
II.	THE EQUATIONS OF MOTION	3
III.	AIRPLANE DATA	9
IV.	RESULTS	16
	APPENDIX A - Details to Part II	22
	APPENDIX B - Influence of an Additional Damping Force	27
	References	29
	Tables	30
	Diagrams	36

I. INTRODUCTION

The three equations of longitudinal motion of an airplane, representing the three degrees of freedom in the plane of symmetry, normally have two pairs of complex roots.

The behavior of a non-spinning missile is described by the same equations, but the character of the motion is different because of the different order of magnitude of some of the coefficients.

For a symmetric missile, a change of the pitching moment due to a perturbation of the longitudinal speed, $\partial M/\partial u$, is equal to zero, and the same is true for the change of the transverse force due to a perturbation of the longitudinal speed, $\partial Z/\partial u$.

This results in an uncoupling of the equations, such that the pitch and transverse motions are independent of longitudinal perturbations and represent the typical short period motion, while the remaining pair of roots, the phugoid mode, degenerates to simple exponential damping.

For most airplanes, $\partial M/\partial u$ also is very small, except in transsonic flight, but $\partial Z/\partial u$ normally must not be neglected. However, contrary to the behavior of most other coefficients, $\partial Z/\partial u$ decreases with increasing flight speed. Therefore, one can expect that in the case of a conventional winged airplane, there exists a certain flight speed at which a similar degeneration of the phugoid occurs.

Theoretical and experimental investigations showed that this point will not be reached during normal operation of conventional airplanes at subsonic speeds. Therefore, it has been undertaken in this investigation to determine the point of phugoid degeneration for super-

sonic and hypersonic flight conditions.

To solve the equations of motion for a conventional airplane at subsonic Mach numbers one usually makes the simplifying assumptions that the airplane is perfectly symmetric and that the concept of small perturbations can be used to linearize the equations. The question whether the validity of these assumptions can be extended to supersonic flight conditions is discussed first.

The investigation then is based on the data of the X-15 research airplane. The X-15 is the only high-speed aircraft whose physical and aerodynamic data are published in some detail. Moreover, its configuration is such that the results obtained in the analysis of the longitudinal motion qualitatively can be adopted for most other supersonic and hypersonic aircraft as well.

II. THE EQUATIONS OF MOTION

General Formulation

The six degrees of freedom of a body in space result in six equations of motion, in which the inertial forces associated with one degree of freedom are balanced by the corresponding aerodynamic and gravity forces. For stability considerations, the equations of motion of a flight vehicle normally are formulated with respect to an orthogonal system of body-fixed stability axes (see Appendix A).

The aerodynamic forces and moments are functions of the motion components, and if the dependence is continuous they can be expressed as Taylor series in terms of these motion variables. Let A be a typical aerodynamic reaction; then the associated Taylor series would be:

$$A = A_0 + \xi \frac{\partial A}{\partial \xi} + \eta \frac{\partial A}{\partial \eta} + \frac{\xi^2}{2} \frac{\partial^2 A}{\partial \xi^2} + \xi \eta \frac{\partial^2 A}{\partial \xi \partial \eta} + \frac{\eta^2}{2} \frac{\partial^2 A}{\partial \eta^2} + \dots \quad (2.1)$$

where ξ and η stand for the deviations of the motion variables from a reference state and for the time derivatives of these deviations on whichever A depends, and all partial derivatives are to be evaluated at the reference point.

Symmetry

Normally, an airplane is designed to be symmetric both geometrically and in its mass distribution, with respect to the x-z plane, defined in Appendix A. This symmetry conceptually admits pure longitudinal motion, i. e., solutions of the equations of motion with the non-symmetric motion components identically equal to zero.

Actually, however, this symmetry of motion is never exact

because of gyroscopic effects, non-symmetries of the airflow, and uneven load distribution. But handling qualities of the airplane require strongly that these coupling effects be kept extremely small, so that for all practical purposes the symmetry of an airplane can be considered as well established.

A first consequence then is that the moments of inertia I_{xy} and I_{yz} vanish. Secondly, all partial derivatives of non-symmetric reactions with respect to longitudinal motion variables must be zero and all first partial derivatives of symmetric reactions with respect to lateral motion variables are also zero (symmetry demands even functions). These conclusions are valid for all steady flight conditions of an airplane with controls fixed. In actual flight tests made to investigate the longitudinal motion of an airplane, the unavoidable lateral motions always can be kept very small by the human or automatic pilot. This results in a very good agreement between the theoretical pure longitudinal solutions and the experimental observations for most flight conditions due to the fact that longitudinal forces and moments arising from lateral deviations can only be of second and higher order in these lateral small perturbations and therefore do not give significant contributions. However, this agreement should not be expected in the transsonic flight regime, since in that case small non-symmetries of the air flow can have large effects on the overall motion of the airplane because of the phenomena associated with the appearance of shocks.

Therefore, for that flight condition, higher order terms must be taken into account in order to predict the behavior of the airplane,

and correspondingly the complete set of equations of motion has to be dealt with.

Outside the transsonic region, both in subsonic and supersonic flight, discontinuities in the aerodynamic forces and moments practically do not occur (except in extreme situations, such as stall), so that for these flight conditions the concept of pure longitudinal motion is appropriate.

Then the equations of motion to be considered for our purposes (longitudinal motion in subsonic, supersonic, and hypersonic flight) become:

$$\begin{aligned} -mg \sin \theta + \Sigma X_{ae} &= m(\dot{u} + qw) \\ mg \cos \theta + \Sigma Z_{ae} &= m(\dot{w} - qu) \\ \Sigma M &= \dot{q} I_y \end{aligned} \tag{2.2}$$

with no dependence of the aerodynamic reactions on lateral motion variables. (X_{ae} , Z_{ae} = aerodynamic forces, M = aerodynamic moments). These equations in general are nonlinear.

Small Perturbation Concept

For subsonic flight, experience showed (see refs. 1 and 2) that in most cases the application of the method of small perturbations from an equilibrium state gives results sufficiently accurate for stability and control considerations.

The restriction to small perturbations implies that all products of disturbance velocities (linear and angular) are of higher order smallness, and terms in which they appear therefore can be neglected. This action linearizes the equations of motion. However, if some of the higher order partial derivatives joined with these products in the

Taylor expansions are very large, then the validity of the linearized equations may possibly be restricted to such small perturbations only, that any actual motion of the airplane would exceed this range of validity. In such a case, nonlinear terms must be taken into account in order to arrive at an agreement between theoretical calculations and flight tests.

The necessary condition for a higher order partial derivative to be very large is that the dependence of the corresponding aerodynamic force on one of the variables be extremely nonlinear in the neighborhood of the reference point.

For the longitudinal aerodynamic forces and moments in supersonic flight, a strong nonlinearity does not exist as long as the airplane under consideration is a conventional one in the sense that it is designed to operate over a certain continuous range of flight conditions and not only at one fixed flight regime, and that the reference conditions lie well inside this operational range.

Under these restrictions, then, the linearization of the equations of motion based on the assumption of small perturbations is permissible, and the obtained results constitute a correct representation of the motion of the airplane.

Final Form of the Equations

With the following notation:

U, θ = steady reference state flight velocity, flight path angle, respectively

u = velocity perturbation in the x-direction

w = velocity perturbation in the z-direction

$w/U = \alpha =$ perturbation in angle of attack

$\vartheta =$ flight path angle perturbation

$q = \dot{\vartheta} =$ angular velocity perturbation about the y-axis

$X =$ x-direction force due to a perturbation

$Z =$ z-direction force due to a perturbation

$M =$ pitching moment due to a perturbation

and eliminating all the steady state forces and moments (they constitute an equilibrium by themselves), the equations to be solved are:

$$m\dot{u} + mg\vartheta \cos \theta - \Sigma X = 0$$

$$m(\dot{w} - U\dot{\vartheta}) + mg\vartheta \sin \theta - \Sigma Z = 0 \quad (2.3)$$

$$I_y \ddot{\vartheta} - \Sigma M = 0$$

Here, the aerodynamic forces, X , Z , and moments, M , are of the form $\xi(\partial A/\partial \xi)_0$, where A denotes one of the aerodynamic reactions, ξ is a disturbance, and the subscript zero indicates that the partial derivative is to be evaluated at the steady reference point. Thus, the equations are simultaneous ordinary differential equations with constant coefficients.

It is convenient to transform these equations into nondimensional form. There are a number of nondimensional systems in use; the one adopted here is the NACA system with $\frac{1}{2}\bar{c}$ (\bar{c} = mean aerodynamic chord) as the characteristic length for longitudinal motion. For details, see Appendix A and ref. 1.

Nontrivial solutions of the expected form $u = u_1 e^{\lambda t}$, $\alpha = \alpha_1 e^{\lambda t}$, $\vartheta = \vartheta_1 e^{\lambda t}$ are possible only if the determinant of coefficients vanishes.

This condition results in the quartic characteristic equation for λ :

$$A\lambda^4 + B\lambda^3 + C\lambda^2 + D\lambda + E = 0$$

whose coefficients are given in Appendix A.

III. AIRPLANE DATA

Description of the Airplane

The phugoid motion of an airplane at supersonic speeds is investigated here using the numerical data of the X-15 research airplane. The X-15 is a rocket-powered, single place airplane designed to investigate the hypersonic flight regime. It has a 5 per cent thick, low aspect ratio, trapezoidal wing mounted in the midposition on a fuselage consisting of a body of revolution with large side fairings. The horizontal tail has a 45° sweep, is all-movable, and may be deflected differentially for roll control. The upper vertical tail is all-movable for directional control, and a fixed lower vertical tail is provided for increased directional stability at high angles of attack and Mach number. Both vertical tails have a 10° single wedge airfoil section.

The flight tests are carried out at Edwards Air Force Base, California. The X-15 is carried under the wing of a B-52 airplane to an altitude of approximately 45,000 feet and released to perform its flight mission. After the rocket fuel is used up, the X-15 glides to a landing on a dry lakebed in the Mohave desert.

In ref. 7 a qualitative description of the airflow associated with the X-15 in supersonic and hypersonic flight is given which indicates that discontinuous changes in the aerodynamic characteristics need not be expected for the flight conditions under consideration.

For the purpose of this investigation, it is assumed that the power plant of the X-15 can be controlled such that the airplane is capable of maintaining a steady horizontal speed at all altitudes. Correspondingly, the airplane weight chosen for the calculations is that

with about half of the fuel capacity left. These assumptions do not represent the actual flight performance of the X-15, which is accelerated by a 1.5 minute run of the rocket engine and then performs most of its test programs in the successive 10 minute power-off gliding flight phase. However, since the aerodynamic characteristics are virtually independent of the power setting of the engine as shown in flight tests (ref. 8), the assumptions made do not restrict the validity of the aerodynamic data.

The physical characteristics of the X-15 airplane as used in this investigation are given in Table 1 and were obtained from ref. 8.

Aerodynamic Characteristics

In ref. 8 the following longitudinal stability derivatives, as determined from flight tests, are given for supersonic Mach numbers up to 3.4:

- C_{N_α} and C_{m_α} , the partial derivatives of the normal force and of the pitching moment coefficient with respect to a change in angle of attack,
- $(C_{m_q} + C_{m_{\dot{\alpha}}})$, the sum of the derivatives of the pitching moment coefficient with respect to the pitching rate $q = \dot{\theta}$ and with respect to the rate of change of the angle of attack.

Using the results of theoretical calculations and of wind tunnel experiments (ref. 7), the values of these derivatives have been estimated up to a Mach number of 8.0. In Figures 1 and 2, the dependence of these derivatives on the Mach number as used in the present investigation is shown (see also Table 3).

The aerodynamic data appearing in the final form of the equations of motion in Appendix A (eqn. A-3) are then obtained as follows.

C_L is the steady flight lift coefficient and can be expressed as:

$$C_L = \frac{W}{S} \frac{1}{\frac{1}{2}\rho U^2} = \frac{W}{S} \frac{1}{\frac{1}{2}\gamma p M^2} = 0.0745 \frac{1}{\frac{p}{p_0} M^2}$$

(for the airplane data used), where

γ = ratio of specific heat at constant pressure to specific heat at constant volume of air,

p = air pressure (p_0 = sea level value) .

C_D is the steady flight drag coefficient which is assumed to be of the form

$$C_D = C_{D_0} + C_L^2 C_{D_1} ,$$

where C_{D_0} and C_{D_1} are functions of the Mach number. Their values have been determined from wind tunnel tests for the Mach numbers 2.29, 2.98, and 4.65 (ref. 6) and have been extrapolated in accordance with theoretical and experimental results for this investigation. In Figure 3, the dependence of C_{D_0} and C_{D_1} on the Mach number is shown as it is used in the calculations.

Using the relations given in Appendix A, the derivatives appearing in the equations of motion can be expressed as:

$$C_{L_\alpha} = C_{N_\alpha} - C_D$$

$$C_{Z_\alpha} = -C_{N_\alpha}$$

$$C_{X_\alpha} = C_L - \frac{\partial C_D}{\partial \alpha} = C_L - 2C_{D_1} C_L C_{L_\alpha}$$

$$C_{X_u} = -2(C_D + C_L \tan \theta) - M \frac{\partial C_D}{\partial M} \quad (\text{in horizontal flight } \theta = 0)$$

$$\begin{aligned}
 C_{Z_u} &= -M \frac{\partial C_L}{\partial M} = -M \frac{\partial(\alpha_o C_{L\alpha})}{\partial M} = -M \frac{C_L}{C_{L\alpha}} \frac{\partial C_{L\alpha}}{\partial M} \\
 &= -M \frac{C_L}{C_{L\alpha}} \left(\frac{\partial C_{N\alpha}}{\partial M} - \frac{\partial C_D}{\partial M} \right) .
 \end{aligned}$$

With the assumed form of the drag coefficient, the derivative $\partial C_D / \partial M$ can be written as

$$\begin{aligned}
 \frac{\partial C_D}{\partial M} &= \frac{\partial C_{D_o}}{\partial M} + C_L^2 \frac{\partial C_{D_1}}{\partial M} + 2C_{D_1} C_L \frac{\partial C_L}{\partial M} \\
 &= \frac{\partial C_{D_o}}{\partial M} + C_L^2 \frac{\partial C_{D_1}}{\partial M} + 2C_{D_1} \frac{C_L^2}{C_{L\alpha}} \left(\frac{\partial C_{N\alpha}}{\partial M} - \frac{\partial C_D}{\partial M} \right) .
 \end{aligned}$$

This can be solved for $\partial C_D / \partial M$:

$$\frac{\partial C_D}{\partial M} = \frac{\frac{\partial C_{D_o}}{\partial M} + C_L^2 \frac{\partial C_{D_1}}{\partial M} + 2C_{D_1} \frac{C_L^2}{C_{L\alpha}} \frac{\partial C_{N\alpha}}{\partial M}}{1 + 2C_{D_1} \frac{C_L^2}{C_{L\alpha}}} .$$

The derivatives $\partial C_{N\alpha} / \partial M$, $\partial C_{D_o} / \partial M$, and $\partial C_{D_1} / \partial M$ were obtained from the figures 1 and 3 by graphical methods (see Table 3).

C_{Z_q} , the change in normal force due to pitch rate, is influenced by both the wing and the horizontal tail, although, when the airplane has a tail the wing contribution to C_{Z_q} is normally small compared to that of the tail. Usually in such cases one increases the tail effect by an amount of the order of 10 per cent to allow for the wing and body. Highly swept or low-aspect-ratio wings may give a more significant contribution to C_{Z_q} , so that for the X-15 it is assumed that:

$$C_{Z_q} = 1.15 (C_{Z_q})_{TAIL}$$

$$\text{with } (C_{Z_q})_{TAIL} = -2 \frac{S_t l_t}{S \bar{c}} (C_{L_\alpha})_{TAIL} \quad (\text{see ref. 1})$$

$$= -2 \times 0.8 (C_{L_\alpha})_{TAIL}$$

$$\text{Then } C_{Z_q} = -1.84 (C_{L_\alpha})_{TAIL}$$

$(C_{L_\alpha})_{TAIL}$, the lift curve slope of the horizontal tail has been obtained from ref. 7 and is plotted over the Mach number in figure 1.

C_{Z_α} , the change in normal force due to rate of change in angle of attack again consists of two parts, the effect of unsteady motion of the wing and the tail effect. The unsteady motion effect on the wing lift can be very important as a forcing term in aeroelastic phenomena but its value is always very small, therefore it is neglected here.

The contribution of the horizontal tail as a good approximation in most cases can be attributed entirely to the fact that the downwash at the tail does not respond instantaneously to changes in wing angle of attack. Using this concept of downwash lag, one obtains:

$$(C_{Z_\alpha})_{TAIL} = -2 \frac{S_t l_t}{S \bar{c}} (C_{L_\alpha})_{TAIL} \frac{\partial \epsilon}{\partial x} \quad (\text{see ref. 1})$$

ϵ = downwash angle at the tail

The wing downwash parameter $\frac{\partial \epsilon}{\partial \alpha}$, as estimated from the charts in ref. 9, is found to be extremely small beyond a Mach number of two. As a consequence, therefore, the derivative C_{Z_α} is neglected completely.

C_{m_u} , the change in pitching moment due to a forward speed perturbation, is of significance only in the transonic regime where the aerodynamic center shifts backward due to the transition of the flow character from subsonic to supersonic. Consequently C_{m_u} can be considered equal to zero outside the transonic region.

In reference 8 the sum of C_{m_q} and $C_{m_{\dot{\alpha}}}$ is given as determined from flight tests. The results of theoretical calculations and of wind tunnel experiments as given in reference 7 show that $C_{m_{\dot{\alpha}}}$ is very small at Mach numbers greater than 3 and is small compared to C_{m_q} at lower speeds.

Furthermore in the characteristic equation, only the sum of C_{m_q} and $C_{m_{\dot{\alpha}}}$ appears in terms of significance, so that it is reasonable to replace C_{m_q} in the equations of motion by the value of $(C_{m_q} + C_{m_{\dot{\alpha}}})$ as given in figure 2 and to put $C_{m_{\dot{\alpha}}} = 0$.

With these relations then and for horizontal flight, i. e. $\theta \equiv 0$, the coefficients of the characteristic equation (A5) for the longitudinal motion of the X-15 airplane finally become

$$\begin{aligned}
 A &= 4\mu^2 i_y \\
 B &= -2\mu i_y (C_{z_a} + C_{x_u}) - 4\mu^2 (C_{m_q} + C_{m_{\dot{\alpha}}}) \\
 C &= i_y (C_{x_u} C_{z_a} - C_{x_a} C_{z_u} + 2C_L C_{x_a}) + 2\mu (C_{m_q} + C_{m_{\dot{\alpha}}}) (C_{z_a} + C_{x_u}) \\
 &\quad - 2\mu C_{m_a} C_{z_q} - 4\mu^2 C_{m_a} \\
 D &= 2\mu C_{x_u} C_{m_a} + C_{x_u} \left[C_{m_a} C_{z_q} - C_{z_a} (C_{m_q} + C_{m_{\dot{\alpha}}}) \right] \\
 &\quad + C_{x_a} (C_{z_u} - 2C_L) (C_{m_q} + C_{m_{\dot{\alpha}}})
 \end{aligned} \tag{3.1}$$

$$E = -C_L C_{m_\alpha} (2C_L - C_{z_u})$$

The arguments used in the evaluation of the derivatives are qualitatively true in general for supersonic airplane configurations, so that the coefficients of the characteristic equation in most cases will be essentially of this form.

IV. RESULTS

Representation and Discussion of the Solutions of the Complete Longitudinal Equations

The three equations of longitudinal motion have been solved numerically for a set of supersonic Mach numbers and different altitudes with the aerodynamic data of the X-15 airplane. The appearing strongly damped, high frequency motion, the so-called "short period mode", not showing any particularities at the flight conditions under consideration and its roots being well remote from the phugoid roots, is ignored in this further discussion.

The obtained roots for the phugoid mode are given in table 5. It can be seen that for high altitudes and moderate supersonic Mach numbers, the roots are complex indicating an oscillatory motion with a tendency to break apart into two aperiodic modes as the altitude decreases or the Mach number increases.

The real part of the roots is plotted over the Mach number for different flight altitudes in figure 4. One observes that:

- (1) The real roots and the real parts of the complex roots are all negative implying that a divergence of a disturbance does not occur.
- (2) As long as the phugoid motion is periodic the value of the real part representing the damping in the system is changing only little with the Mach number and is decreasing with increasing altitude.
- (3) Once degenerated into two aperiodic modes, one of these real roots increases in magnitude with increasing Mach number or decreasing flight altitude, representing a pure convergence, while the other root asymptotically approaches zero.

The observations (2) and (3) are confirmed in figure 5, showing the location of the phugoid roots in the complex plane for the flight altitudes 20,000 ft., 40,000 ft., and 60,000 ft. The imaginary part of the roots, representing the frequency of the motion goes down with increasing Mach number, while the real part remains almost constant until the root locus reaches the real axis. From then on one root rapidly approaches zero and the other root increases along the negative real axis.

Phugoid Approximation

In the attempt to arrive at a closed form criterion for the phugoid degeneration, the simplifying concept of the phugoid approximation has been applied.

Noting that the dimensionless coefficients for the airplane mass and for the moment of inertia, μ and i_y , are very large numbers, one realizes that the coefficients A, B and C in the characteristic equation [eqs. (A6) or (3.1)] are very large compared to the coefficients D and E.

Consequently then there must exist large roots dependent essentially on the values of A, B and C, and small roots determined approximately by the second order equation which results from neglecting the first two terms of the characteristic equation.

Retaining only the dominant terms in the last three coefficients one finds for the small phugoid roots the characteristic equation

$$-4\mu^2 C_{m_a} \lambda^2 + 2\mu C_{x_u} C_{m_a} \lambda - (2C_L^2 - C_L C_{z_u}) C_{m_a} = 0$$

and since $C_{m_\alpha} \neq 0$ for statically stable airplanes

$$-4\mu^2 \lambda^2 + 2\mu C_{x_u} \lambda - 2C_L^2 + C_L C_{z_u} = 0 \quad (4.1)$$

A different approach leading to the same approximation of the phugoid is the following:

Expecting the phugoid roots to be very small, i. e. the phugoid motion to be very slow, then the pitch rate and the acceleration in pitch are going to be vanishingly small. But the pitching moment equation then requires α , the angle-of-attack disturbance, also to be extremely small, since C_{m_α} is one of the larger derivatives.

Therefore an approximation for the phugoid motion would be obtained by putting $\alpha = 0$.

This is equivalent to assuming a very large value for C_{m_α} , the restoring moment, such that the angle of attack remains virtually constant during the phugoid motion.

As a consequence then the third equation of the set (A3) can be dropped (since $C_{m_\alpha} \approx 0$) and the remaining equations are, for horizontal flight ($\theta = 0$),

$$(2\mu D - C_{x_u}) \hat{u} + C_L \delta = 0$$

$$(2C_L - C_{z_u}) \hat{u} - 2\mu D \delta = 0 \quad (C_{z_q} \text{ neglected})$$

The corresponding characteristic equation is

$$-4\mu^2 \lambda^2 + 2\mu C_{x_u} \lambda - 2C_L^2 + C_L C_{z_u} = 0$$

and this is identical with equation (4.1).

The roots of this extremely simplified characteristic equation have been computed for the same flight conditions as before. The results are in very good agreement with the solutions of the complete set of equations of longitudinal motion. The accuracy of the phugoid

approximation is found to be within 2% for most of the calculated points.

Therefore any information obtained from the simple phugoid approximation can be used with reasonable justification to describe the actual behavior of the airplane in the investigated Mach number and altitude range.

This statement should be valid in general, since in coming to this point no qualitative arguments have been used which are true specifically only for the X-15 airplane and not for most other conventional configurations as well.

Derivation of a Criterion for the Phugoid Degeneration

The characteristic equation of the phugoid approximation then provides a criterion for the degeneration of the normally periodic phugoid motion into two aperiodic modes.

The roots of the quadratic equation (4.1) will be real if:

$$4\mu^2 C_{x_u}^2 \geq 4.4\mu^2 (2 C_L^2 - C_L C_{z_u})$$

With the identities

$$C_{x_u} = -2 C_D - M \frac{\partial C_D}{\partial M}$$

$$C_{z_u} = -M \frac{C_L}{C_{L_a}} \cdot \frac{\partial C_{L_a}}{\partial M}$$

the condition becomes:

$$C_D^2 \left(2 + \frac{M}{C_D} \frac{\partial C_D}{\partial M} \right)^2 \geq 4 C_L^2 \left(2 + \frac{M}{C_{L_a}} \frac{\partial C_{L_a}}{\partial M} \right)$$

i. e.
$$\frac{C_L}{C_D} \leq \frac{2 + \frac{M}{C_D} \frac{\partial C_D}{\partial M}}{2 \left(2 + \frac{M}{C_{L\alpha}} \frac{\partial C_{L\alpha}}{\partial M} \right)^{\frac{1}{2}}}$$

Condition for the phugoid degeneration to occur.

As the Mach number goes to zero this criterion approaches the form $\frac{C_L}{C_D} \leq \frac{1}{\sqrt{2}} = 0.707$ which is in agreement with the known condition for critical damping, $\frac{C_L}{C_D} = \frac{1}{\sqrt{2}}$, for the phugoid motion of a conventional airplane in incompressible air flow. Therefore the criterion given here can be considered valid over the whole Mach number range starting from zero, except for the transonic region.

Using the aerodynamic data of the X-15 airplane, the critical value of C_L/C_D as given above has been computed for all flight conditions under consideration, and in addition the value of C_L/C_D which corresponds to a trimmed steady flight of the X-15 under the same conditions has been obtained. The results are given in table 6 and plotted in figure 6.

In the limiting value of C_L/C_D the only variation with altitude appears in the lift depending part of C_D . Since the lift coefficient C_L is very small at nearly all considered flight conditions this variation is extremely small and therefore the limiting value of C_L/C_D marking the degeneration of the phugoid is practically independent of the flight altitude and a function only of the Mach number.

Comparing figures 6 and 4 one observes that the points of intersection in figure 6 lie at the same Mach numbers at which in figure 4 the splitting of the roots occurs. This confirms the good agreement

of the degeneration criterion with the exact solutions of the equations of motion.

Figure 6 indicates that at supersonic flight speeds at sea level the phugoid mode is not likely to occur as the normal oscillatory motion. However any economic operation of an airplane requires a value of the ratio C_L/C_D greater than 3 at least, so that in all normal supersonic as well as subsonic flight conditions the phugoid mode appears as a low frequency periodic motion.

APPENDIX A

Stability Axes

To describe the motion of a flight vehicle, in most cases Newton's second law is expressed with respect to stability axes, i. e. a body fixed orthogonal coordinate system x, y, z , with its origin at the aircraft center of gravity, the x -axis pointing forward in the direction of the initial steady flight velocity, the z -axis pointing downward and the y -axis pointing out the right wing such that the $y = 0$ plane coincides with the plane of symmetry of the airplane.

The General Equations of Motion

Denoting the scalar components of the linear velocity along the x, y , and z axes by u, v , and w and the scalar components of the angular velocity about the x, y , and z axes by p, q , and r , the motion of a rigid airplane with controls fixed is described by the set of equations:

$$\left. \begin{aligned} \Sigma X &= m (\dot{u} + qw - rv) \\ \Sigma Y &= m (\dot{v} + ru - pw) \\ \Sigma Z &= m (\dot{w} + pv - qu) \end{aligned} \right\} \quad (\text{A. 1a})$$

$$\left. \begin{aligned} \Sigma L &= \dot{p}I_x + (rp - \dot{q})I_{xy} - (\dot{r} + pq)I_{zx} + (r^2 - q^2)I_{yz} + qr(I_z - I_y) \\ \Sigma M &= \dot{q}I_y + (pq - \dot{r})I_{yz} - (\dot{p} - qr)I_{xy} + (p^2 - r^2)I_{zx} + rp(I_x - I_z) \\ \Sigma N &= \dot{r}I_z + (qr - \dot{p})I_{xz} - (\dot{q} + rp)I_{yz} + (q^2 - p^2)I_{xy} + pq(I_y - I_x) \end{aligned} \right\} \quad (\text{A. 1b})$$

Here m is the mass of the airplane, the I 's are the moments of inertia, defined by $I_x = \int_A (y^2 + z^2) dm$, $I_{xz} = \int_A xz dm$, etc.,

X , Y , and Z are the external forces, consisting of aerodynamic (including propulsive) and gravity forces, in the x , y , and z directions and L , M , and N are the external aerodynamic moments about the x , y , and z axes respectively.

Denoting the orientation of the body fixed coordinate system with respect to an earth fixed system x_e, y_e, z_e ($x_e y_e$ - plane = horizontal plane, x_e pointing forward in the nominal flight direction) in the usual way by the angles ψ (aximuth), θ (pitch), and ϕ (roll), the gravity forces take the form

$$X_g = -mg \sin\theta \quad Y_g = mg \cos\theta \sin\phi \quad Z_g = mg \cos\theta \cos\phi$$

Nondimensionalization of the Equations of Motion and Final Form

To transform the equations of motion into nondimensional form the following procedure has been applied:

The aerodynamic forces are expressed as $F = \frac{1}{2} \rho V^2 S C_F$
and the aerodynamic moments as $M = \frac{1}{2} \rho V^2 S \bar{c} C_M$

where

ρ = density of the air, \bar{c} = mean aerodynamic cord, S = wing area, $V^2 = (U + u)^2 + v^2 + w^2$

In the case of pure longitudinal motion $v = 0$.

The derivatives of the forces and moments with respect to a perturbation ξ become:

$$\left(\frac{\partial F}{\partial \xi}\right)_0 = F_{\xi} = \rho V S C_F \left(\frac{\partial V}{\partial \xi}\right)_0 + \frac{1}{2} \rho V^2 S \left(\frac{\partial C_F}{\partial \xi}\right)_0 \quad (\text{A. 2})$$

$$\left(\frac{\partial M}{\partial \xi}\right)_0 = M_{\xi} = \rho V S \bar{c} C_M \left(\frac{\partial V}{\partial \xi}\right)_0 + \frac{1}{2} \rho V^2 S \bar{c} \left(\frac{\partial C_M}{\partial \xi}\right)_0$$

The perturbations ξ are made dimensionless using U as divisor for velocity perturbations and $\frac{2U}{\bar{c}}$ for angular rate perturbations.

The time is nondimensionalized by $t^* = \frac{\bar{c}}{2U}$, i. e. $t = \hat{t} t^* = \hat{t} \frac{\bar{c}}{2U}$, and derivatives with respect to the nondimensional time \hat{t} are denoted by D , i. e. $\frac{d}{d\hat{t}} = D = t^* \frac{d}{dt}$.

The stability derivatives $C_{F_{\xi}}$ and $C_{M_{\xi}}$ then represent partial derivatives of the force and moment coefficients C_F and C_M with respect to the nondimensional form $\hat{\xi}$ of the perturbation ξ .

Further the mass of the airplane is expressed as $m = \mu \frac{\rho S \bar{c}}{2}$ and the moment of inertia about the y-axis as $I_y = i_y \frac{\rho S \bar{c}^3}{8}$ (see table 2).

The transformation results in the nondimensional equations

$$(2\mu D - 2C_{L \tan \theta} - C_{x_u}) \hat{u} - C_{x_a} a + C_L \vartheta = 0$$

$$(2C_L - C_{z_u}) \hat{u} + (2\mu D - C_{z_a} D - C_{z_a}) a - (2\mu D + C_{z_q} D - C_L \tan \theta) \vartheta = 0$$

$$- C_{m_u} \hat{u} - (C_{m_a} D + C_{m_a}) a + (i_y D^2 - c_{m_q} D) \vartheta = 0$$

where all derivatives with respect to acceleration quantities, except C_{z_a} and C_{m_a} , are neglected as is C_{x_q} , because these are normally very small compared to the other derivatives. Clearly, when it appears necessary to do so, any of the terms dropped can be restored into the equations without difficulty.

Assuming solutions of the form $\hat{u} = \hat{u}_1 e^{\lambda t}$, $\alpha = \alpha_1 e^{\lambda t}$, $\vartheta = \vartheta_1 e^{\lambda t}$ one arrives at the characteristic equation

$$\begin{vmatrix} (2\mu\lambda - C_{x_u}) & -C_{x_\alpha} & C_L \\ 2C_L - C_{z_u} & (2\mu\lambda - C_{z_\alpha} \lambda - C_{z_\alpha}) & -(2\mu + C_{z_q})\lambda \\ -C_{m_u} & -(C_{m_\alpha} \lambda + C_{m_\alpha}) & (i_y \lambda^2 + C_{m_q} \lambda) \end{vmatrix} = 0 \quad (\text{A.4})$$

Here it is assumed that the reference condition is horizontal flight, i. e. $\theta = 0$.

The expansion of the determinant leads to a quartic equation for λ :

$$A \lambda^4 + B \lambda^3 + C \lambda^2 + D \lambda + E = 0$$

the roots of which give the desired information about the motion of the airplane.

The coefficients of the characteristic equation are:

$$A = 2\mu i_y (2\mu - C_{z_\alpha})$$

$$B = 2\mu i_y (C_{z_\alpha} + C_{x_u}) + i_y C_{x_u} C_{z_\alpha} - 2\mu (C_{z_q} C_{m_\alpha} - C_{m_q} C_{z_\alpha}) - 4\mu^2 (C_{m_\alpha} + C_{m_q})$$

$$C = i_y (C_{x_u} C_{z_\alpha} - C_{x_\alpha} C_{z_u}) + 2\mu (C_{z_\alpha} C_{m_q} - C_{m_\alpha} C_{z_q} + C_{x_u} C_{m_q} + C_{x_u} C_{m_\alpha}) - 4\mu^2 C_{m_\alpha} - C_{x_u} (C_{m_q} C_{z_\alpha} - C_{z_q} C_{m_\alpha}) + 2 C_L C_{x_\alpha} i_y \quad (\text{A.6})$$

$$D = 2C_L^2 C_{m_\alpha} + 2\mu [C_{x_u} C_{m_\alpha} - (C_{x_\alpha} - C_L) C_{m_u}] + C_{x_u} (C_{m_\alpha} C_{z_q} - C_{m_q} C_{z_\alpha}) - C_{x_\alpha} (C_{m_u} C_{z_q} - C_{m_q} C_{z_u}) - C_L (C_{m_u} C_{z_\alpha} - C_{z_u} C_{m_\alpha}) - 2C_L C_{m_q} C_{x_\alpha}$$

$$E = -C_L [C_{m_\alpha} (2C_L - C_{z_u}) + C_{m_u} C_{z_\alpha}]$$

Usually one wants to express the derivatives of the force coefficients C_x and C_z in terms of the lift, drag, and thrust coefficients.

With the assumption that the thrust vector is aligned with the x-axis and for small angles of attack α the following relations can easily be verified:

$$C_x = C_T + C_L \alpha - C_D$$

$$C_z = -C_L - C_D \alpha$$

The thrust T is assumed to be independent of the motion variables for rocket and jet propulsion systems.

APPENDIX B

The most efficient way to increase the damping of the phugoid motion in subsonic flight is to apply an additional longitudinal force by controlling the thrust proportional to $(-u)$ or to α , both of which have approximately the same phase.

To show the effect of such a damping force on the phugoid in supersonic flight, an additional u -dependent term has been introduced into the x -force equation.

Denoting the damping thrust force by $F_D = C_F \frac{1}{2}\rho U^2 S$ with

$$\begin{aligned} C_F &= C_{DF} \cdot \frac{u}{U^2} \\ &= \frac{C_{DF}}{U} \cdot \hat{u} , \end{aligned}$$

then a constant C_{DF} corresponds to a thrust force proportional to u , independent of U . The x -force equation then reads:

$$\left(2\mu D - C_{x_u} - \frac{C_{DF}}{U} \right) \hat{u} - C_{x_\alpha} \alpha + C_L \vartheta = 0 .$$

The equations of motion have been solved with C_{DF} taking the values 30 and 300 in addition to the case without artificial damping, $C_{DF} = 0$.

The effect of an increase of this damping term is essentially the same as a decrease in flight altitude: the real part of the phugoid is slightly increased compared to the undamped case as long as the roots are complex, the degeneration point occurs at a smaller Mach number, and the successive departure of the two real roots is more extreme, one of them going to zero and the other increasing with increasing Mach number.

In Figure 7, the real part of the roots is plotted over the Mach number for a flight altitude of 40,000 ft. In this case, the dependence of the results on the additional damping is most obvious, but the tendency is the same at all other altitudes.

Considering the additional damping C_{DF}/U as an increase of C_{x_u} and noting that the main contribution to C_{x_u} comes from the drag coefficient C_D , then the introduction of the damping term can be thought of as an increase of the drag coefficient, where $C_{DF} = 30, 300$ corresponds to an increase of C_{x_u} by a factor of approximately 1.2, 2.2, respectively.

Thus, the application of a damping thrust control reduces the lift to drag ratio C_L/C_D as it appears in the criterion for phugoid degeneration, see Part IV, bringing its value closer to the limiting value.

It should be noted, however, that the lift to drag ratio based on the actual airplane shape and flight condition is not changed by the additional damping term.

REFERENCES

1. B. Etkin, Dynamics of Flight, John Wiley and Sons, New York (1959).
2. E. Seckel, Stability and Control of Airplanes and Helicopters, Academic Press, New York (1964).
3. H. Schlichting, E. Truckenbrodt, Aerodynamik des Flugzeuges, Vol. 2, Springer (1960).
4. U. S. A. F., Stability and Control Datcom., October 1960 (revised Nov. 1965).
5. R. S. Osborne, "Aerodynamic Characteristics of a 0.067-Scale Model of the N. A. X-15 Research Airplane at Transonic Speeds," NASA TM X-24 (Sept. 1959).
6. A. E. Franklin, R. M. Lust, "Investigation of the Aerodynamic Characteristics of a 0.067-Scale Model of the X-15 Airplane at Mach Numbers of 2.29, 2.98, and 4.65," NASA TM X-38 (Nov. 1959).
7. H. J. Walker, C. H. Wolowicz, "Theoretical Stability Derivatives for the X-15 Research Airplane at Supersonic and Hypersonic Speeds Including a Comparison with Wind Tunnel Results," NASA TM X-287 (Aug. 1960).
8. R. B. Yancey, H. A. Rediess, G. H. Robinson, "Aerodynamic Derivative Characteristics of the X-15 Research Airplane as Determined from Flight Tests for Mach Numbers from 0.6 to 3.4," NASA TN D-1060 (Jan. 1962).
9. R. C. Haefeli, H. Mirels, J. L. Cummings, "Charts for Estimating Downwash behind Rectangular, Trapezoidal, and Triangular Wings at Supersonic Speeds," NACA TN 2141 (Aug. 1950).

TABLE 1

X-15, AIRPLANE DATA

WEIGHT	$W = 22,000 \text{ lbs.}$ (This includes 7,400 lbs. fuel.)
TOTAL WING AREA	$S = 200 \text{ sq. ft.}$
WING LOADING	$\frac{W}{S} = 100 \frac{\text{lbs.}}{\text{sq. ft.}}$
MEAN AERODYNAMIC CHORD	$\bar{c} = 10.27 \text{ ft.}$
"TAIL VOLUME"	$\frac{S_t l_t}{S \bar{c}} = 0.55 \cdot 1.46 = 0.8$ $S_t =$ horizontal tail area $l_t =$ distance from airplane c. g. to mean aerodynamic center of the horizontal tail
MOMENT OF INERTIA	$I_y = 95,000 \text{ slug ft}^2.$
CONSIDERED SPEED RANGE:	Mach 1.25 - 8.0
CONSIDERED FLIGHT ALTITUDE:	Sea level 20,000 ft. 40,000 ft. 60,000 ft.

TABLE 2

X-15, MASS AND MOMENT OF INERTIA PARAMETERS

$$\begin{aligned} \mu &= \frac{m}{\rho S \frac{c}{2}} = \frac{W}{S} \cdot \frac{2}{g \cdot c} \cdot \frac{1}{\rho_0} \cdot \frac{1}{\rho/\rho_0} \\ &= 280.5 \frac{1}{\rho/\rho_0} \end{aligned}$$

$$\begin{aligned} i_y &= \frac{I_y}{\rho S (\frac{c}{2})^3} = \frac{8I_y}{S \cdot c^3} \cdot \frac{1}{\rho_0} \cdot \frac{1}{\rho/\rho_0} \\ &= 1472 \cdot \frac{1}{\rho/\rho_0} \end{aligned}$$

	Sea level	20,000 ft.	40,000 ft.	60,000 ft.
ρ/ρ_0	1	0.4595	0.1851	0.07078
ρ/ρ_0	1	0.5328	0.2462	0.09414
μ	280.5	526.0	1140	2980
i_y	1472	2760	5980	15630

TABLE 3

AERODYNAMIC DATA OF THE X-15

Mach	$C_{N\alpha}$	$\frac{\partial C_{N\alpha}}{\partial M}$	C_{D_0}	$\frac{\partial C_{D_0}}{\partial M}$	C_{D_1}	$\frac{\partial C_{D_1}}{\partial M}$	$C_{m\alpha}$	$(C_{m_g} + C_{m\dot{\alpha}})$
1.25	4.6	01.925	0.0575	0	0.23	0.052	-1.63	-14.2
1.5	4.1	-1.75	0.057	-0.003	0.25	0.073	-1.67	-9.2
2.0	3.33	-1.31	0.055	-0.006	0.29	0.111	-1.43	-5.1
3.0	2.34	-0.64	0.047	-0.008	0.417	0.114	-0.85	-3.0
4.0	1.9	-0.29	0.040	-0.0056	0.52	0.092	-0.57	-2.4
5.0	1.7	-0.167	0.035	-0.0044	0.60	0.072	-0.43	-2.1
6.0	1.55	-0.120	0.0315	-0.0035	0.67	0.057	-0.35	-2.0
7.0	1.43	-0.090	0.028	-0.0028	0.718	0.046	-0.28	-1.9
8.0	1.33	-0.075	0.026	-0.0024	0.76	0.0375	-0.225	-1.8

TABLE 4

X-15, LIFT AND DRAG COEFFICIENTS FOR TRIMMED HORIZONTAL FLIGHT

Mach	Sea level		20,000 ft.		40,000 ft.		60,000 ft.	
	C_L	C_D	C_L	C_D	C_L	C_D	C_L	C_D
1.25	0.0477	0.058	0.1038	0.060	0.258	0.073	0.674	0.162
1.5	0.0331	0.057	0.0721	0.058	0.179	0.065	0.468	0.112
2.0	0.0186	0.055	0.0405	0.056	0.1006	0.058	0.263	0.075
3.0	0.0083	0.047	0.0180	0.047	0.0448	0.048	0.117	0.053
4.0	0.0047	0.040	0.0101	0.040	0.0252	0.040	0.0658	0.042
5.0	0.0030	0.035	0.0065	0.035	0.0161	0.035	0.0421	0.036
6.0	0.0021	0.0315	0.0045	0.0315	0.0112	0.032	0.0293	0.032
7.0	0.0015	0.028	0.0033	0.028	0.0082	0.028	0.0215	0.028
8.0	0.0012	0.026	0.0025	0.026	0.0063	0.026	0.0165	0.026

TABLE 5
PHUGOID ROOTS OF THE X-15

Mach	Sea Level			20, 000 ft.			40, 000 ft.			60, 000 ft.		
	Real	Imaginary		Real	Imaginary		Real	Imaginary		Real	Imaginary	
1.25	-0.02108	-0.03490	0	-0.01412	0.02610		-0.006861	0.03135		-0.00477	0.03194	
1.5	-0.00879	-0.05496	0	-0.01595	0.01782		-0.007332	0.02465		-0.00407	0.02549	
2.0	-0.00338	-0.07285	0	-0.01050	-0.02742	0	-0.008402	0.01615		-0.00384	0.01782	
3.0	-0.00134	-0.08012	0	-0.00339	-0.03702	0	-0.008805	0.008187		-0.00364	0.01146	
4.0	-0.000814	-0.08854	0	-0.00199	-0.04231	0	-0.009611	0.002113		-0.00386	0.00905	
5.0	-0.000538	-0.09253	0	-0.00130	-0.04483	0	-0.00426	-0.01570	0	-0.00393	0.00718	
6.0	-0.000361	-0.09736	0	-0.000864	-0.04755	0	-0.00258	-0.01833	0	-0.00407	0.00555	
7.0	-0.000257	-0.09854	0	-0.000615	-0.04833	0	-0.00176	-0.01936	0	-0.00409	0.00419	
8.0	-0.000199	-0.10155	0	-0.000473	-0.04993	0	-0.00134	-0.02040	0	-0.00419	0.00313	

TABLE 6
 $\left(\frac{C_L}{C_D}\right)_{\text{CRITICAL}}$ AND $\left(\frac{C_L}{C_D}\right)_{\text{TRIM}}$ FOR THE X-15

Mach	Sea Level		20,000 ft.		40,000 ft.		60,000 ft.	
	Critical	Trim	Critical	Trim	Critical	Trim	Critical	Trim
1.25	0.822	0.822	0.811	1.731	0.757	3.543	0.620	4.161
1.50	0.823	0.578	0.818	1.237	0.784	2.753	0.662	4.188
2.0	0.814	0.338	0.812	0.730	0.800	1.736	0.739	3.504
3.0	0.687	0.176	0.687	0.382	0.685	0.937	0.671	2.220
4.0	0.609	0.116	0.609	0.253	0.609	0.625	0.611	1.557
5.0	0.558	0.085	0.558	0.185	0.558	0.458	0.561	1.167
6.0	0.537	0.066	0.537	0.143	0.538	0.354	0.539	0.912
7.0	0.528	0.054	0.528	0.118	0.528	0.293	0.529	0.758
8.0	0.502	0.045	0.502	0.097	0.502	0.242	0.503	0.628

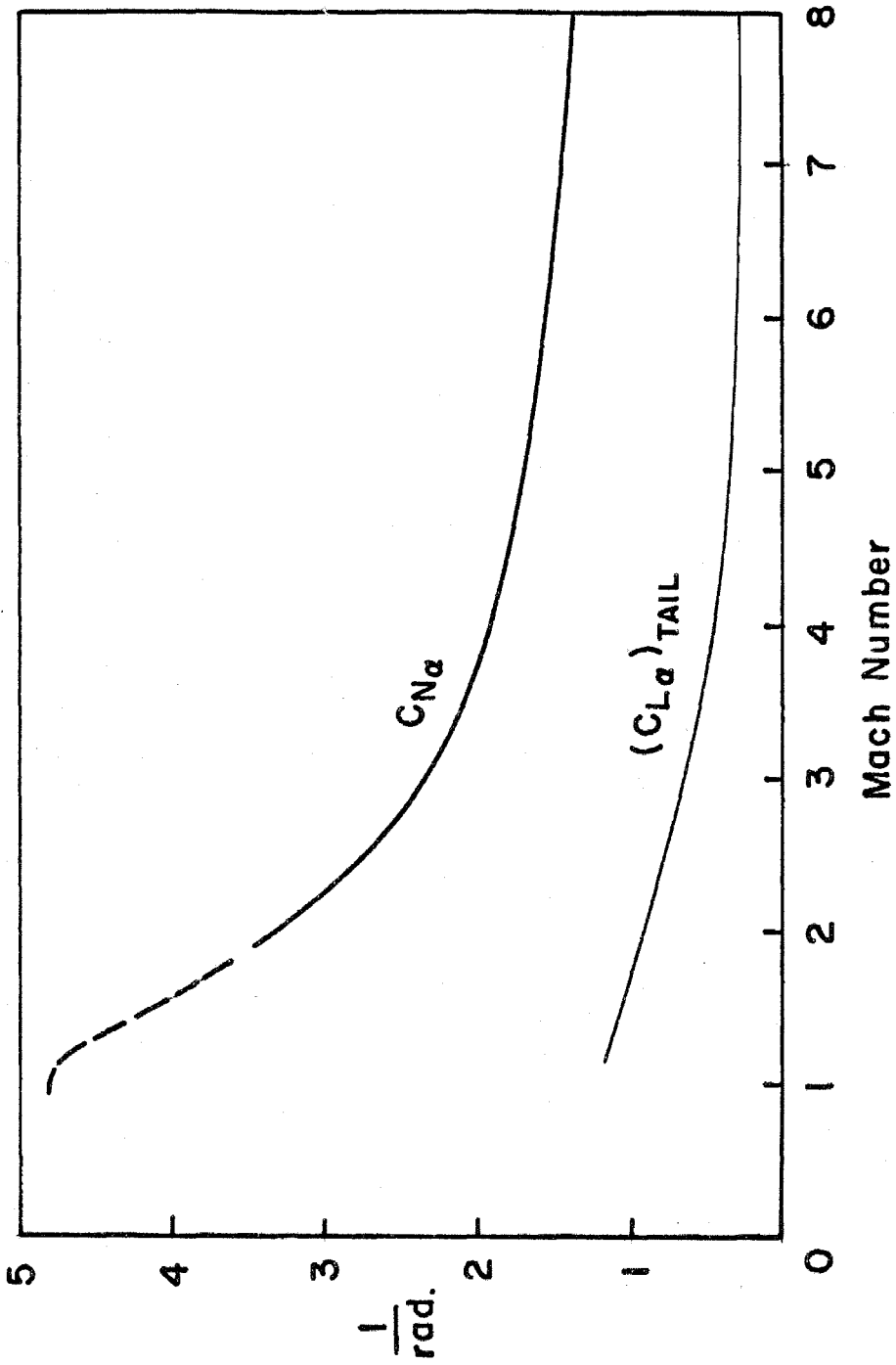


FIG. 1a $C_{N\alpha}$ AND $(C_{L\alpha})_{\text{TAIL}}$ AS FUNCTIONS OF THE MACH NUMBER

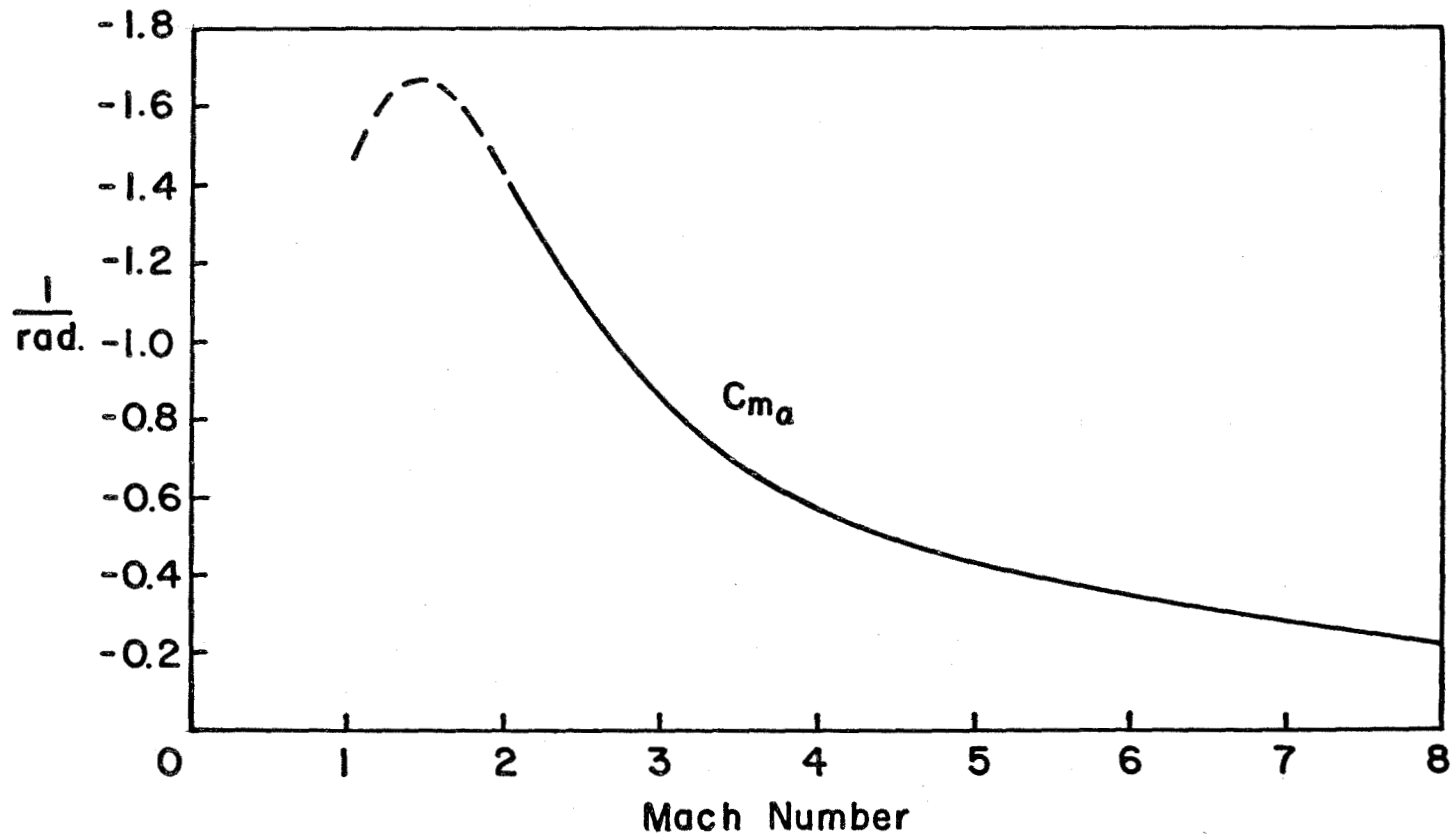


FIG. 1b $C_{m\alpha}$ AS A FUNCTION OF THE MACH NUMBER

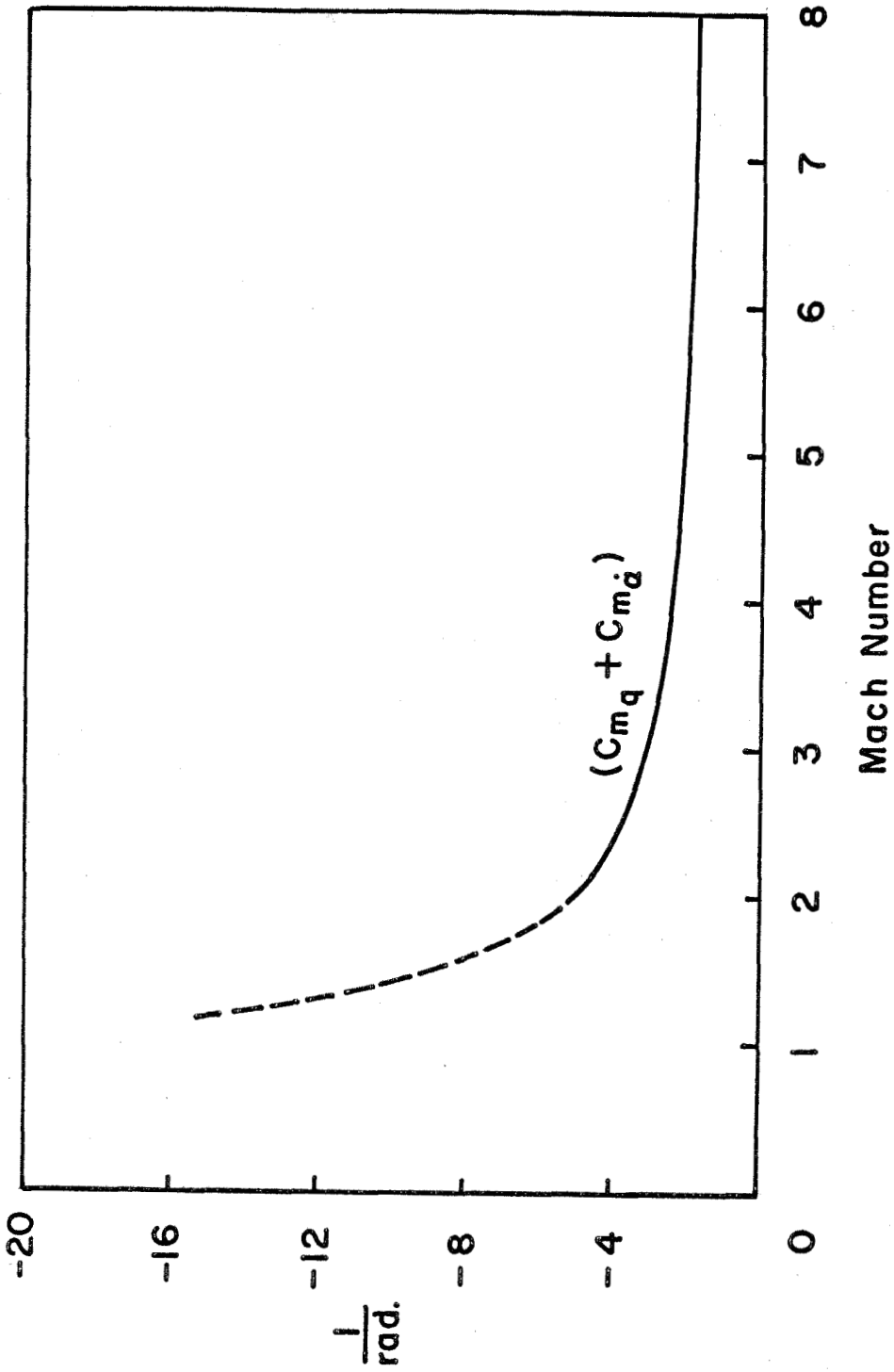


FIG. 2 DAMPING IN PITCH, $(C_{m_q} + C_{m_{\dot{\alpha}}})$, AS A FUNCTION OF THE MACH NUMBER

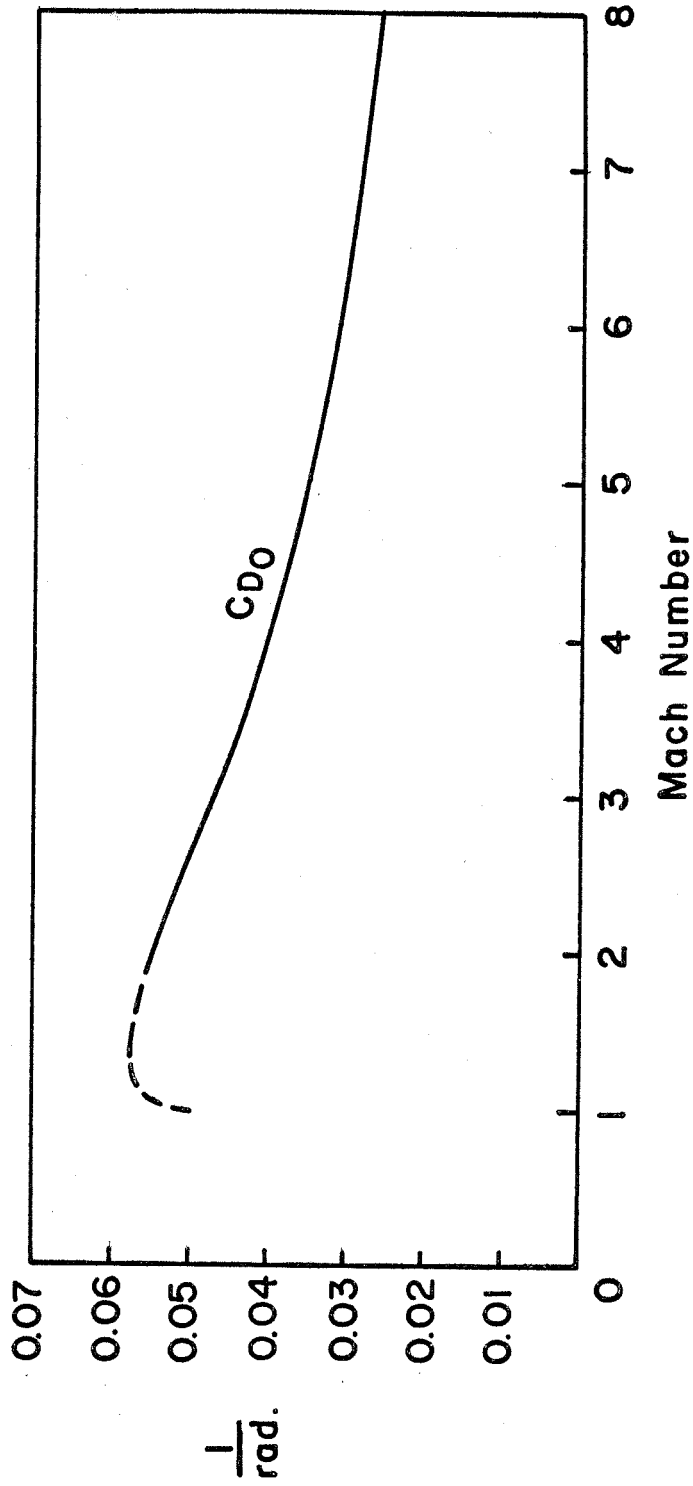


FIG. 3a THE DRAG PARAMETER C_{D0} AS A FUNCTION OF THE MACH NUMBER

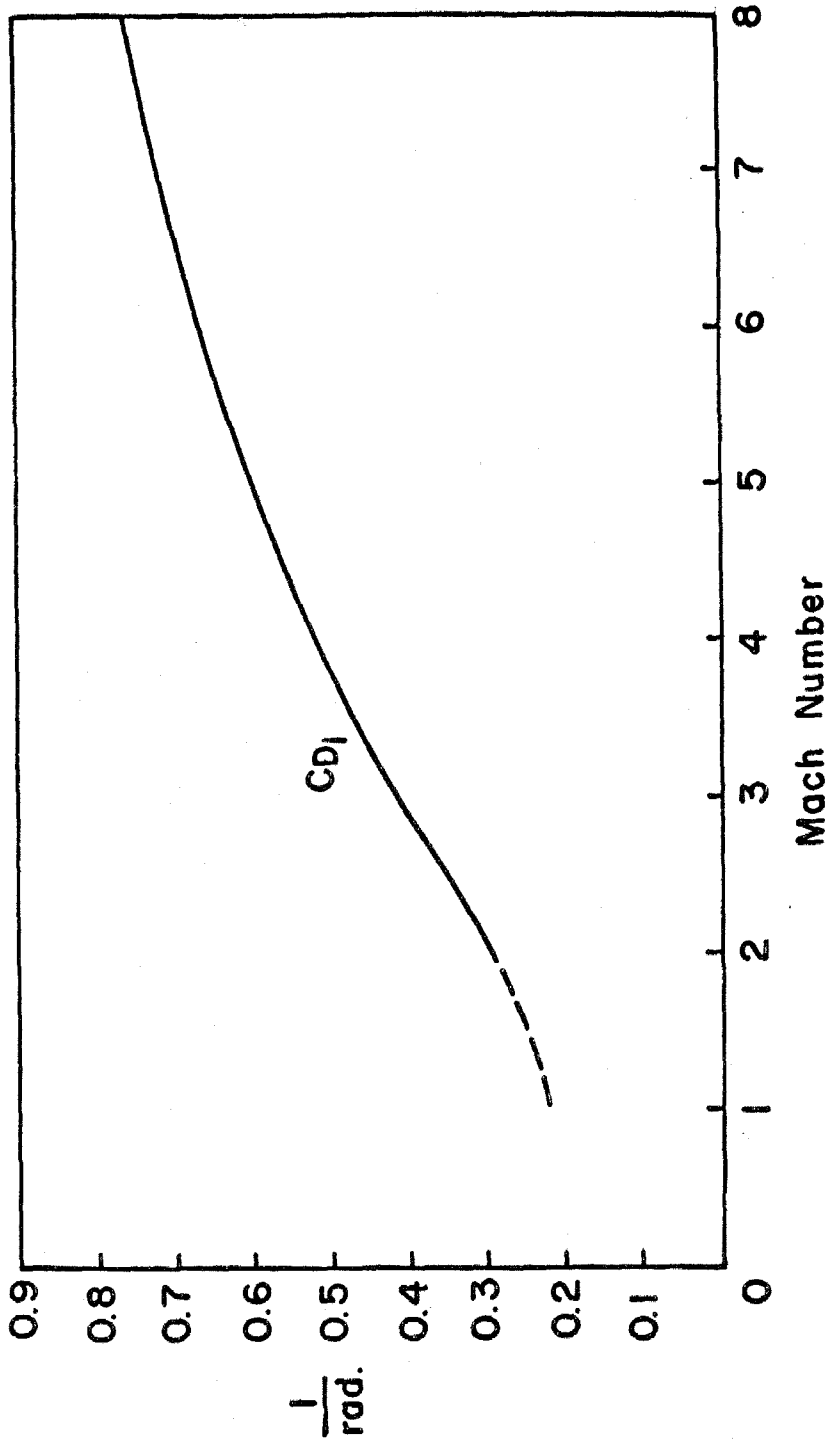


FIG. 3b THE DRAG PARAMETER CD_j AS A FUNCTION OF THE MACH NUMBER

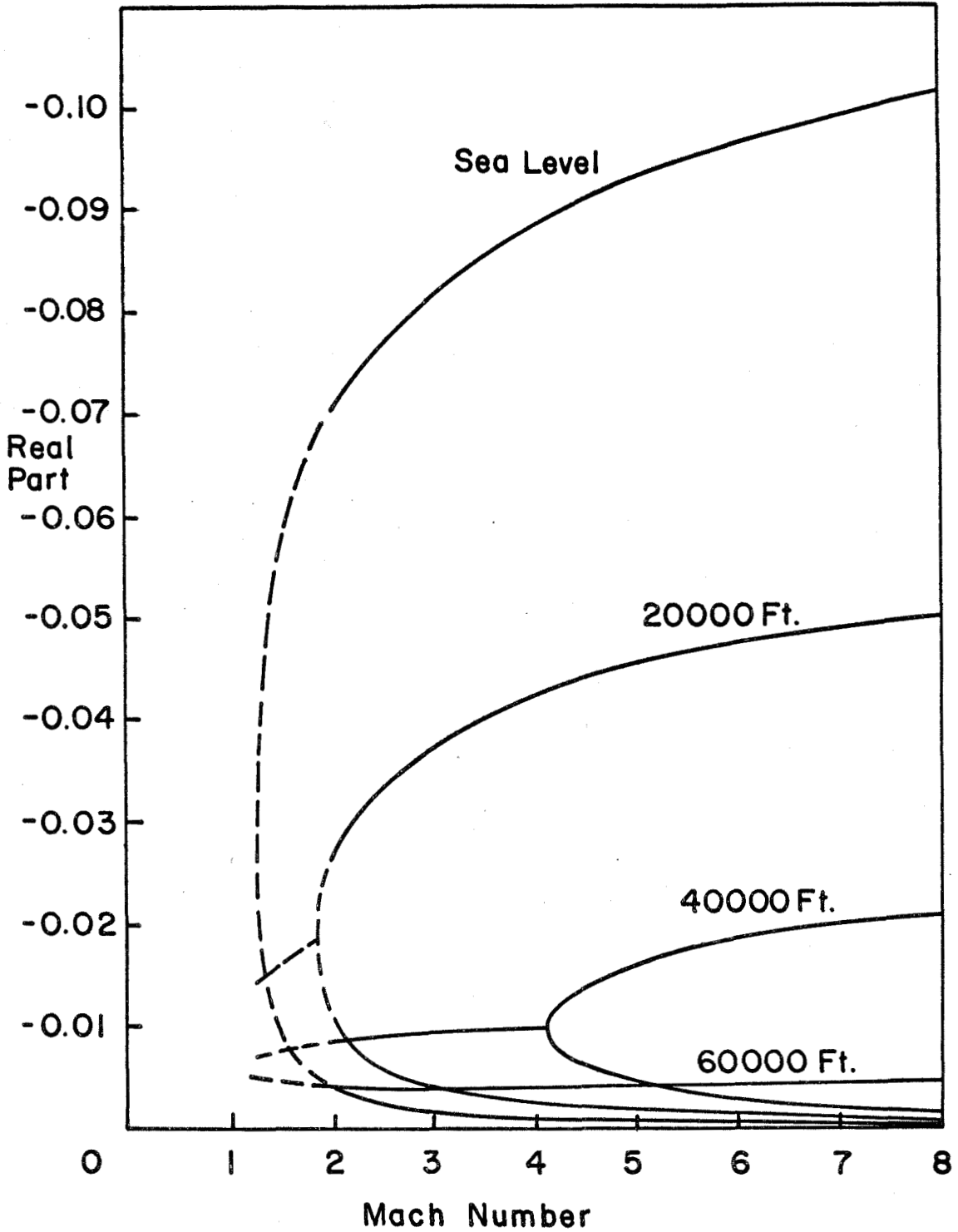


FIG. 4 REAL PART OF THE PHUGOID ROOTS FOR DIFFERENT FLIGHT ALTITUDES

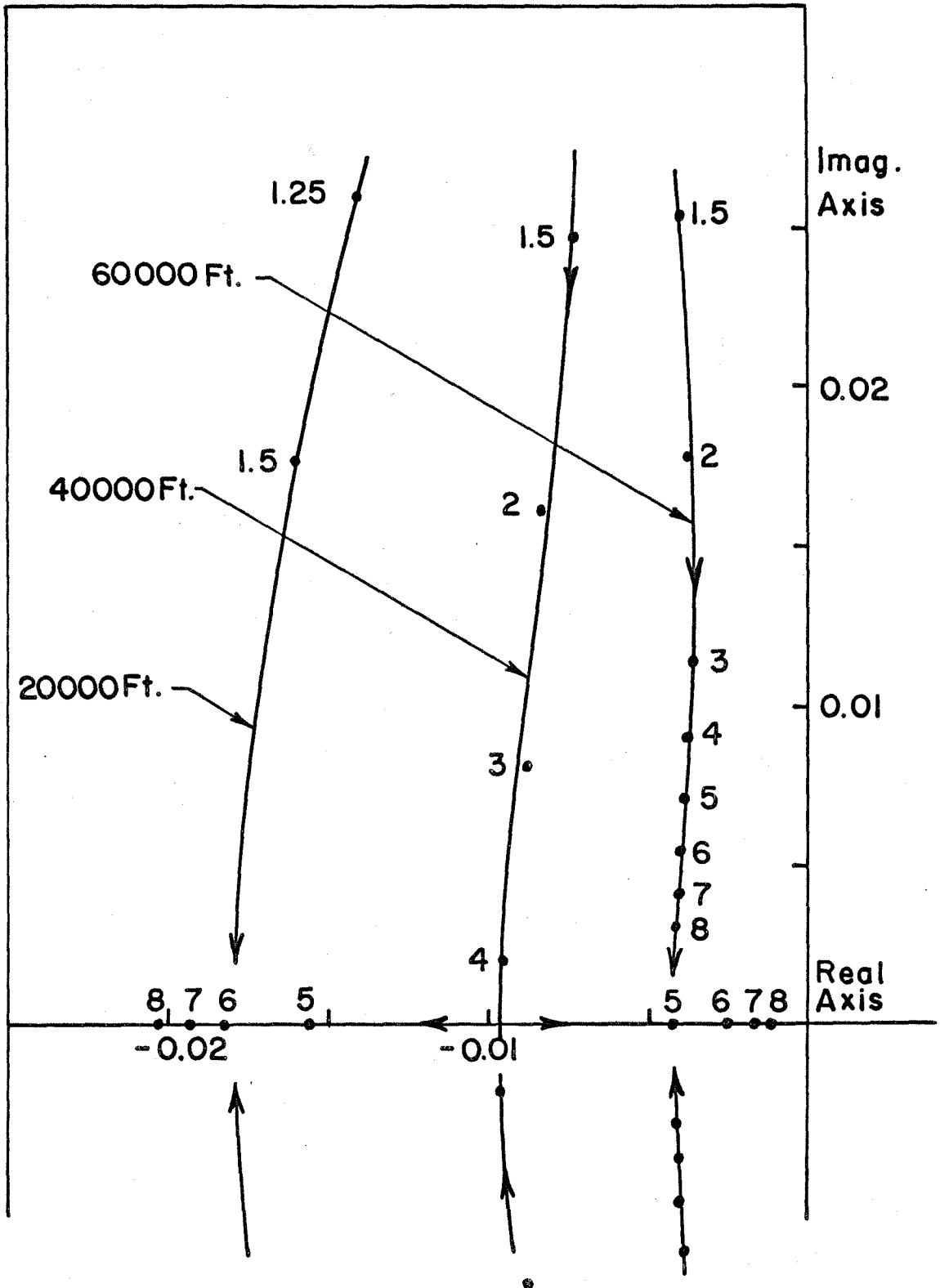


FIG. 5 THE PHUGOID ROOTS SHOWN IN THE COMPLEX PLANE

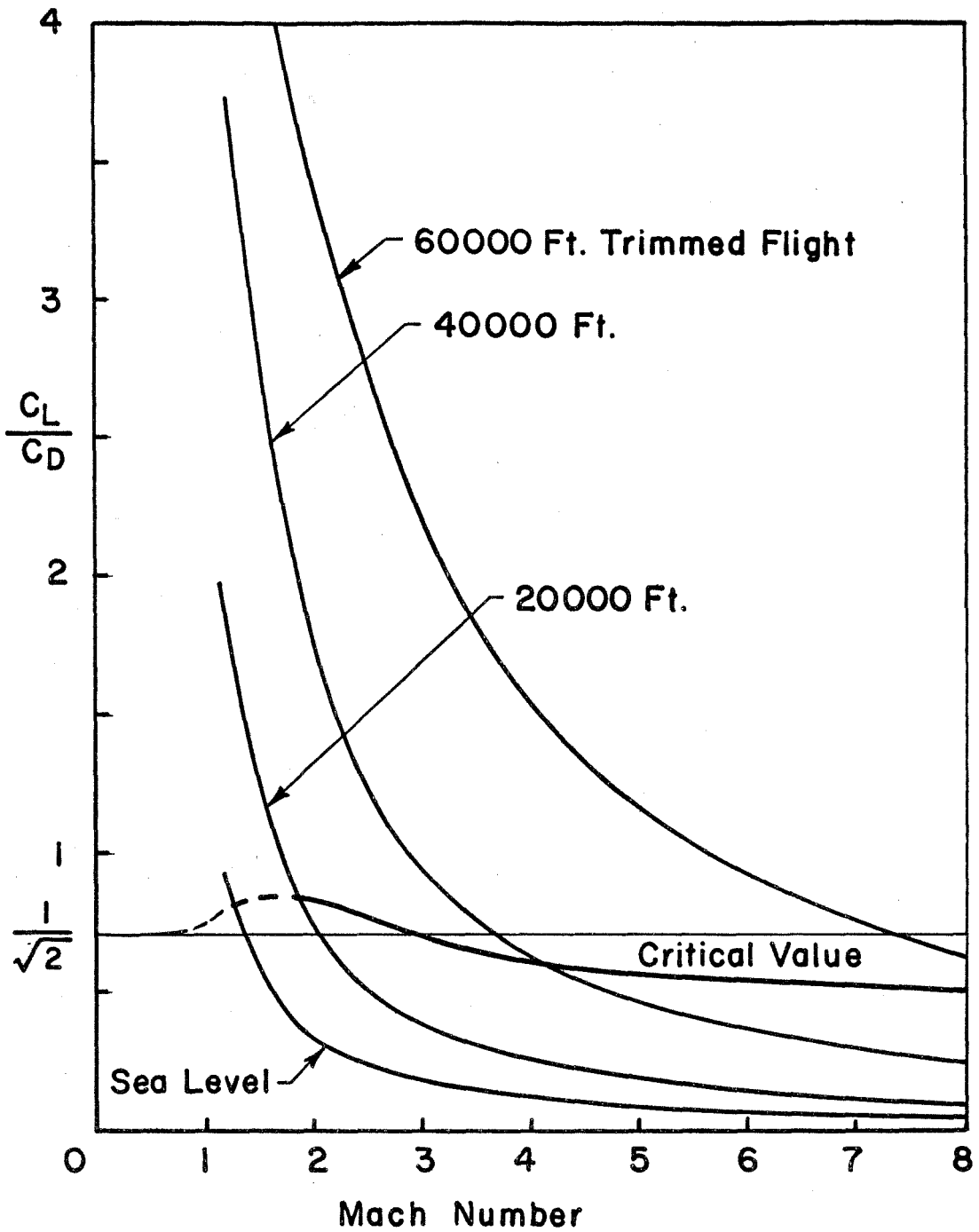


FIG. 6 LIFT TO DRAG RATIO OF THE X-15
(TRIMMED FLIGHT AND CRITICAL VALUE)

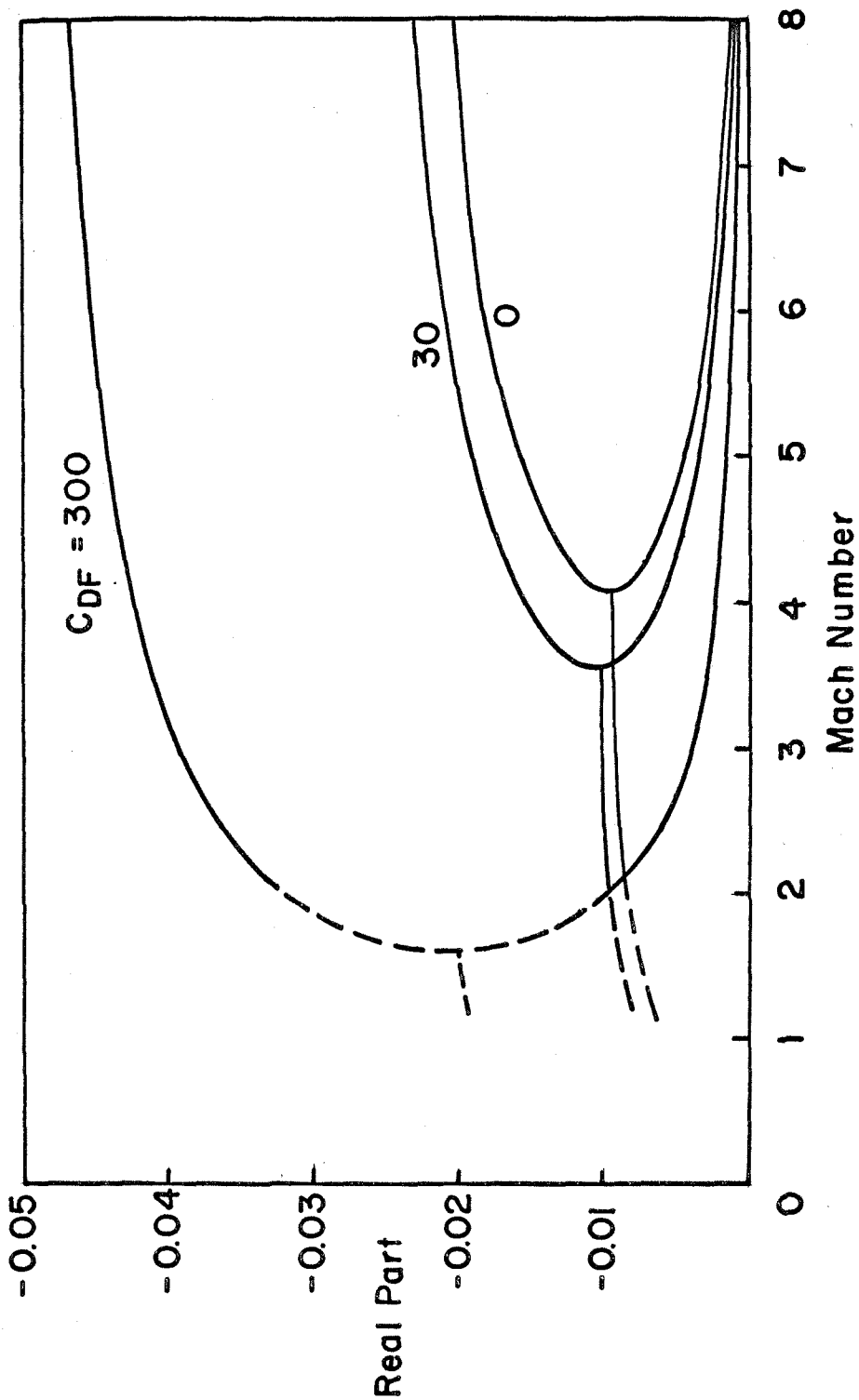


FIG. 7 INFLUENCE OF AN ADDITIONAL DAMPING FORCE ON THE REAL PARTS OF THE PHUGOID ROOTS (ALTITUDE 40000 FT.)